JOURNAL OF SPACECRAFT AND ROCKETS
Vol. 41, No. 5, September–October 2004

Unsteady Gasdynamics Effects in Pyrotechnic Actuators

Hobin S. Lee*
Scot, Incorporated, Downers Grove, Illinois 60515

Unsteady flow effects in pyrotechnic actuators are examined quantitatively and are shown to significantly affect the performance of a pyrotechnic device when the function time or the stroke time of the device is in the order of a characteristic gasdynamics timescale of the product gases in the device. A one-dimensional "purely" gasdynamics model is developed to simulate the unsteady effects in a closed-bomb firing and in a normally open pyrotechnic valve. The model results are compared to test data and are found to agree well with the data. The results of the gasdynamics model are also compared with those of a quasi-equilibrium model, and the limitations of both models are investigated. Consequently, a nondimensional time parameter τ_c is established, which can be used to approximate the level of unsteady effect on the total energy output of a given pyrotechnic device. It is concluded that the unsteady effects can be neglected with a reasonable degree of accuracy when $\tau_c > 1$.

Nomenclature

A_P = effective piston area, in.^{2} (m^2)
a = piston acceleration, ft^2/s (m^2/s)
b = burning-rate slope coefficient in Eq. (11), in./s/psi^n (m/s/Pa^n)
c = sound speed, ft/s (m/s)
c_r = reference sound speed, ft/s (m/s)
c_s = initial shock sound speed, ft/s (m/s)
$\bar{c}_v$ = average constant volume coefficient of heat, ft-lbf/lbm/(J/kg/K)
D_i = effective internal diameter of actuator, in. (cm)
dx = grid spacing, in. (cm)
E = total energy, ft-lbf (J)
e = total specific energy, ft-lbf/lbm (J/kg)
$\bar{f}$ = average wall-friction coefficient
k_j = jth polynomial coefficient for form function in Eq. (12)
L = reference duct length, in. (cm)
M_p = piston mass, lbm (kg)
m_{cv} = mass of gases in control volume, lbm (kg)
m_p = mass of combustion product gases, lbm (kg)
m_{p0} = total mass of energetic material, lbm (kg)
n = burning-rate power constant in Eq. (11)
P = pressure, psi (Pa)
P_{CB} = specified peak pressure of an initiator when fired in a closed bomb, psi (Pa)
P_d = initial pressure downstream of initiator closure disk, psi (Pa)
$P_{R.W.}$ = pressure at right-hand-side wall, psi (Pa)
P_r = reference pressure, psi (Pa)
P_s = initial shock pressure, psi (Pa)
P_u = initial pressure upstream of initiator closure disk, psi (Pa)
P_0 = initial pressure, psi (Pa)
$\dot{Q}$ = total heat-transfer rate, ft-lbf/s (W)
$\dot{q}$ = heat-transfer rate per unit mass, ft-lbf/s/lbm (W/kg)
$\bar{R}$ = average gas constant, ft-lbf/lbm/R (J/kg/K)
S = total stroke distance, in. (cm)
T = temperature, K
t = time, s
u = fluid velocity, ft/s (m/s)
V = volume, in.^{3} (cm^2)
V_{CB} = closed-bomb volume in which the specified peak-pressure of an initiator is given, in.^{3} (cm^3)
V_0 = initial internal volume of actuator, in.^{3} (cm^3)
υ = specific volume, in.^{3}/lbm (m^3/kg)
υ_d = specific volume downstream of closure disk, in.^{3}/lbm (m^3/kg)
υ_u = specific volume upstream of closure disk, in.^{3}/lbm (m^3/kg)
υ_0 = initial specific volume, in.^{3}/lbm (m^3/kg)
W = work, ft-lbf (J)
$\dot{W}$ = power, ft-lbf/s (W)
W_s = initial shock speed, ft/s (m/s)
x = Eulerian space coordinate, in. (cm)
x_i = location of closure disk, in. (cm)
x_{s0} = initial location of piston face, in. (cm)
α = bulk wall-friction coefficient ratio
γ = ratio of specific heats
$\bar{\eta}$ = average covolume, in.^{3}/lbm (m^3/kg)
λ = web distance of propellant grain, in. (m)
ξ = Lagrangian space coordinate
ξ_R = location of piston face in Lagrangian space coordinate
ρ = density, lbm/in.^{3} (kg/m^3)

Received 21 May 2003; presented as Paper 2003-4530 at the AIAA/ASME/SAE/ASEE 39th Joint Propulsion Conference, Huntsville, AL, 20–23 July 2003; revision received 8 September 2003; accepted for publication 9 September 2003.

*Senior Analyst, Ballistics Analysis, 2525 Curtiss Street. Member AIAA.

Introduction

PYROTECHNIC actuators are mechanical devices that are powered by energy released from chemical reactions in energetic materials. They are relatively compact in size but are capable of delivering high mechanical power output and have a long-term storage life that is usually longer than 10 years. This feature makes them an optimum choice for aerospace applications that require a lightweight device providing sufficient mechanical energy in a short period of time as well as a long shelf life. Typically pyrotechnic actuators are used as subcomponents to provide pulling, cutting, or thrusting mechanisms that are critical to the entire mission and the safety of the flight. For example, Figs. 1 and 2 are photographs of just two devices among the 400-plus pyrotechnic components that fly on each shuttle mission. Figure 1a is the emergency thruster designed to deploy the shuttle's main landing gear in the case of the hydraulics failure. Figure 1b is the thruster's cartridge containing the explosive materials used to provide the thrust energy, ignited by two NSI-1 initiators.[1] Figure 2 is a photograph of the pin-puller, also initiated by two NSI-1 initiators, used as a part of the drag parachute release mechanism, which is executed during every shuttle landing. Figure 3 is a photograph of a pyrotechnic valve that is used to shut off the engine of a satellite launch vehicle by cutting off the fuel

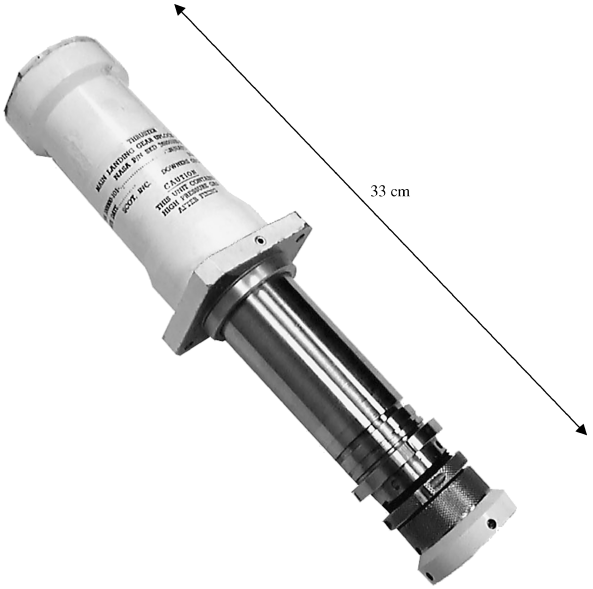

Fig. 1a Photograph of pyrotechnic thruster used for an emergency landing scenario for the space shuttle.

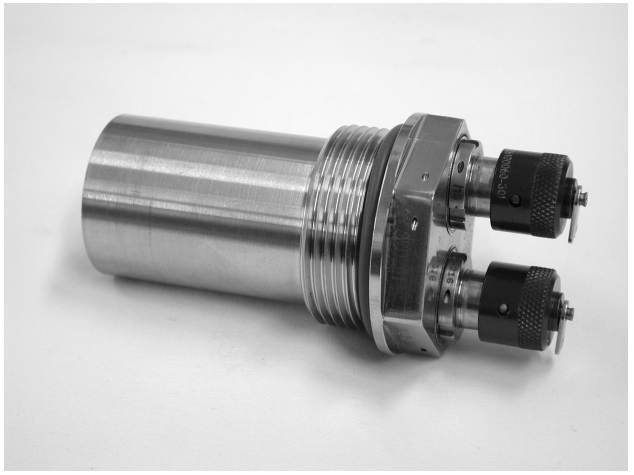

Fig. 1b Photograph of explosive cartridge used in the pyrotechnic thruster.

flow. A good summary and a brief history of pyrotechnic devices are given in Ref. 2.

The function of a pyrotechnic actuator is essentially described by linear displacement of a boundary, aided by energy produced by the chemical reactions in explosives, either in the form of detonation-produced kinetic energy, or potential energy of the combustion product gases, or a combination of both. Therefore, the mechanical energy output of a pyrotechnic actuator is directly related to the detonation/deflagration characteristics of the energetic materials used. For this reason, the mechanical aspects of pyrotechnic devices must be designed in conjunction with design of the explosives. When estimating the mechanical energy output produced by a pyrotechnic actuator, a common practice is to assume a quasi-equilibrium process in which the thermodynamic quantities in the device are spatially homogeneous at any time interval for the duration of entire stroke. This allows for a model that consists of a system of ordinary differential equations with respect to time, which can be solved with relative ease.[3–7] The quasi-equilibrium assumption usually yields good results except when the function time or the total stroke time of the device is in the order of the characteristic gasdynamics timescale of the combustion product gases in the device. In such cases, the spatial gradients of thermodynamic quantities must be accounted for because the pressure at the moving boundary can vary significantly from the quasi-equilibrium value

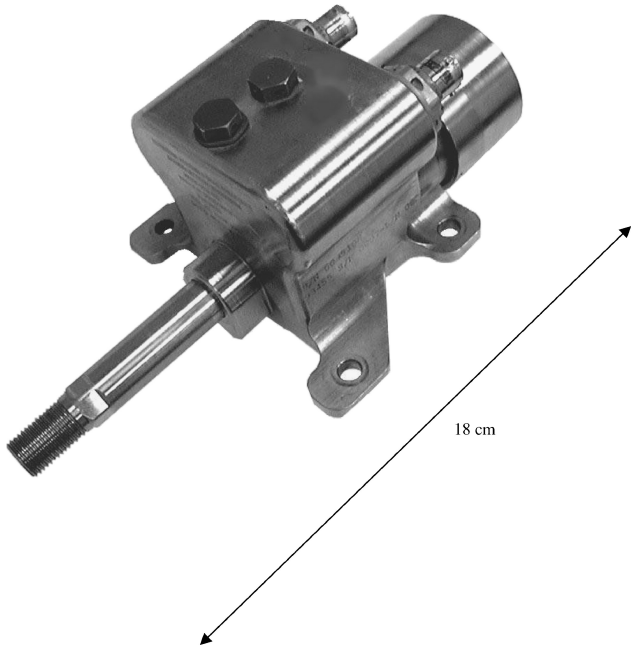

Fig. 2 Photograph of pyrotechnic pin-puller used for drag parachute deployment during the space shuttle landing.

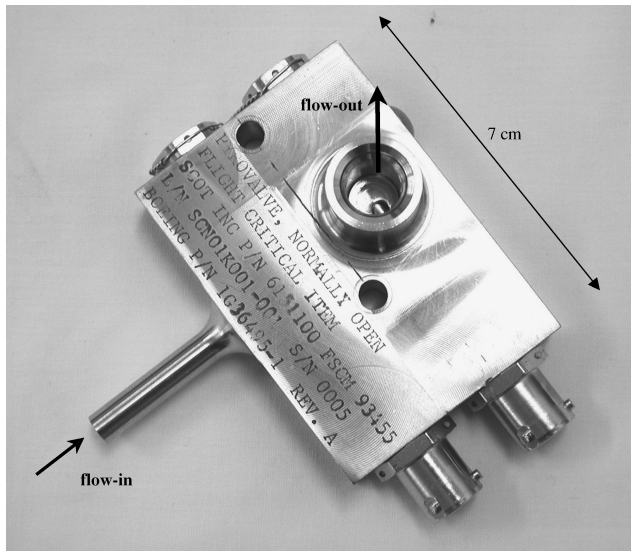

Fig. 3 Photograph of normally open pyrotechnic valve used for engine shutoff of a satellite launch vehicle.

at a given moment during stroke.[8] Therefore, unsteady effects can play a significant role in determining the reliability of a pyrotechnic device.[9]

In the present study, the unsteady gasdynamics effects are first illustrated by examining closed-bomb test results of the NASA Standard Initiator, Type 1 (NSI-1) initiator. The unsteady effects are further examined by utilizing a one-dimensional unsteady gasdynamics model, which solves transient compressible flow problems with moving and/or rigid boundaries. The model is then applied to simulate performance of a normally open pyrotechnic valve. Finally, the model is used to establish a nondimensional time parameter that can be used to determine when and whether the quasi-equilibrium approximation will be valid for a given device.

Initiator Performance

NSI-1 Initiator in 10-cc Closed Bomb

Initiator performance is usually specified by its peak pressure value in a closed bomb. For example, the NSI-1 is specified to produce 650 ± 125 psi (4480 ± 860 kPa) in a 10-cc bomb.[10] There is,

however, a level of ambiguity in this usual way of specifying initiator performance because it does not address the unsteady pressure fluctuation that is present in the initiation process. A typical initiation mechanism of a bridgewire initiator is as follows: 1) electrical current is applied to bridgewire, 2) bridgewire heats up and ignites the primary charge surrounding it, 3) primary charge ignites the main charge, 4) pressure increases in the initiator housing as a result of hot combustion products, and 5) closure disk ruptures allowing combustion products to flow out into the void volume of the closed bomb. The closure disk initially separates the region of high-pressure gases in the initiator housing from the quiescent region downstream, thereby creating a pressure discontinuity. And when the closure disk ruptures, it essentially sets up a shock flow. The flow upstream of the pressure discontinuity consists of the combustion products and possibly a portion of main charge still burning, and the flow downstream consists of undisturbed air/gas in the bomb. Immediately following the rupturing of the closure disk, pressure at any location in the bomb will exhibit unsteady characteristics as a result of wave interactions until a steady state is reached. During the unsteady phase, the fluctuating pressure in the bomb might well exceed the maximum value specified or fall below the minimum. Therefore, it must be assumed that the peak pressure value used to specify the initiator performance must correspond to the pressure value at the instant when unsteady waves disappear and a steady state begins.

Figure 4 shows a pressure–time trace of NSI-1 fired in a 10-cc closed bomb. The pressure–time trace is acquired via a piezoelectric pressure gauge with 100-KHz sampling rate. The piezoelectric gauge is a PCB Piezotronics pressure transducer, Model 113A23, which has a range of 10 kpsi (68,950 kPa) with a resolution of 0.2 psi. The calibration certification provided by the manufacturer gives the uncertainty of measurement of $\pm 1\%$ based on a level of confidence of approximately 95%. A Hi-Techniques data-acquisition system, HT600, is used to obtain and store the electric signals from the transducer into a digital format. The analog-to-digital card used for the system had the capacity of 2-μs minimum sampling interval and the 12-bit (or 0.024%) resolution.[11]

As shown in Fig. 4, the pressure-time trace exhibits two distinct phases. The first phase is characterized by high-amplitude fluctuation, which indicates strong wave interactions. The second phase of the pressure trace is characterized by a relatively smooth decrease in pressure with time as a result of heat loss, which indicates that the thermodynamic quantities in the bomb have reached a steady state. During the first phase, the absolute maximum pressure reaches above 1500 psi (10340 kPa), while the absolute minimum pressure is as low as 250 psi (1720 kPa). The point where the unsteady phase gives way to the steady phase is best interpolated to occur at 0.38 ms from the first indication of pressure; the pressure at that point is 680 psi (4690 kPa), which is well within the specified value for NSI-1.

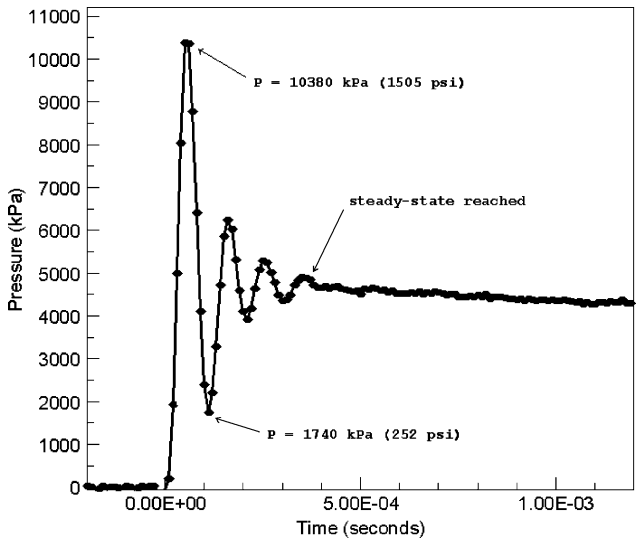

Fig. 4 Pressure vs time trace of NSI-1 initiator firing in 10-cc closed bomb.

The pressure–time trace illustrates the ambiguity of the commonly used method of specifying an initiator's performance. Even though the interpolated peak pressure value at the start of a steady-state phase is within the specified limits, the absolute peak value is well above the upper limit. One can assume that the specification limits are applied to the steady portion of the data, which might be appropriate for most cases. If, however, the initiator were to be used in an application in which the unsteady phase plays a significant role, then it is important to understand and specify the initiator's performance in a matter that addresses the unsteady portion of its output.

Gasdynamics Model

To further understand the significance of the unsteady effect, a one-dimensional gasdynamics model is considered. The equations that comprise the model are conservation of mass, momentum equation, energy equation, and the equation of state.[12] They are expressed here in a Lagrangian coordinate system. The heat and momentum diffusion terms are neglected, but a bulk momentum loss as a result of wall friction and a bulk heat loss to surrounding are added as source terms. Even though the combustion products most likely do not behave like ideal gases, an ideal gas equation of state is used because it is assumed that the nonideal gas effects are small. The governing equations described here represent a purely gasdynamic model in that they do not include equations of burning or detonation for explosives. The model assumes an instantaneous burnout of the explosives; therefore, the combustion or detonation aspect of the pyrotechnic device is considered through the initial condition of the problem. The governing equations are shown here.

Continuity:

$$\frac{\partial v}{\partial t} - \frac{\partial u}{\partial \xi} = 0 \tag{1}$$

Momentum:

$$\frac{\partial u}{\partial t} + \frac{\partial p}{\partial \xi} = -\alpha u^2 \tag{2}$$

Energy:

$$\frac{\partial e}{\partial t} + \frac{\partial}{\partial \xi}(u \cdot p) = \dot{q} \tag{3}$$

where

$$\xi = \int^{x} \rho(x')\,\mathrm{d}x' \tag{4}$$

The total energy e is defined as

$$p = \rho(\gamma - 1)(e - u^2/2) \tag{5}$$

The source term in the momentum equation $-\alpha u^2$ is a bulk loss caused by wall friction, where α is defined by the ratio $\bar{f}/2D_i$. The value of $\bar{f}$ is estimated by using the Moody Chart and the Reynolds number based on the internal diameter of the device, an average kinematic viscosity of the combustion product gases, and the initial shock fluid velocity in the device.[13] The heat loss $\dot{q}$ is also given as a bulk loss across a control volume. In general, it is a difficult task to predict the heat loss accurately, but a semi-empirical scheme can be devised with the available test data. In many cases, a pyrotechnic device completes its function quick enough so that the conductive/convective heat loss through the device's housing can be modeled as a heat-transfer problem in a semi-infinite solid with surface convection. Then the problem reduces to a matter of estimating a correct convective heat-loss coefficient.[14] A detail treatment of heatloss approximation in a pyrotechnic retractor is illustrated in Ref. 4. These equations are solved numerically by the piecewise parabolic method, which is a well established method for solving

strong shock problems.[11] The initial and boundary conditions are described in Eqs. (6–8).

Initial conditions:

$$\upsilon(0,\xi) = \upsilon_0(x), \qquad P(0,\xi) = P_0(x), \qquad u(0,\xi) = 0 \quad (6)$$

$$P_0,\, \upsilon_0(x) = \begin{cases} P_u, \upsilon_u & x \le x_i \\ P_d, \upsilon_d & x. > x_i \end{cases} \quad (7)$$

Boundary conditions:

$$\upsilon,\, P(t,0) = \text{Rigid-wall shock reflection condition}$$

$$u(t,0) = 0, \qquad u(t,\xi_R) = \frac{A_p}{M_p}\int P_{\text{R.W.}}\, \mathrm{d}t \quad (8)$$

Figure 5 is a schematic diagram of a pyrotechnic device and the initial pressure profile used by the gasdynamics model. Even though the schematic diagram shows an actuator with a piston, it can easily be used to model a closed bomb by assigning an infinite mass to the piston, thus rendering it a rigid wall. At time zero, the initial thermodynamic quantities follow the pressure profile described in Eq. (6), which is a step function with the discontinuity located at the initiator closure disk interface x_i. This implies that the model assumes an instantaneous burnout of the initiator charge. The boundary conditions in Eq. (7) represent a rigid, reflecting wall at the left-hand side and a moving (or stationary) piston at the right. P_u is calculated so that it is consistent with the specific pressure specified for the initiator. For example, a NSI-1 initiator will yield

$$P_u = (650\,\text{psi}) \cdot (10\,\text{cc}) \Big/ \left(\pi x_i D_i^2/4\right) \quad (9)$$

where $(\pi x_i D_i^2/4)$ is the internal volume of the initiator housing. The model also assumes that the closure disk is a mass-less diaphragm such that at time $= 0^+$ the fluid upstream of discontinuity flows downstream with no restrictions, setting up a planar shock traveling to right. In reality, the flow is three-dimensional, and the closure disk might rupture before or after the energetic material completely burns out. The three-dimensional effect is not investigated in this study, even though it may be a nonnegligible factor. However, the timing effect of charge burnout vs the disk rupture can heuristically be considered with the one-dimensional model described herein by simply changing the value of x_i. The case when the charge burns out much more locally, that is, in a smaller volume than the total available internal volume of initiator housing, can be simulated by decreasing x_i, which will yield higher P_u. Similarly, the case when the charge burns slowly so that its burnout occurs after the disk rupture can be simulated by increasing x_i, which will yield lower P_u. This timing effect will be further investigated in subsequent sections.

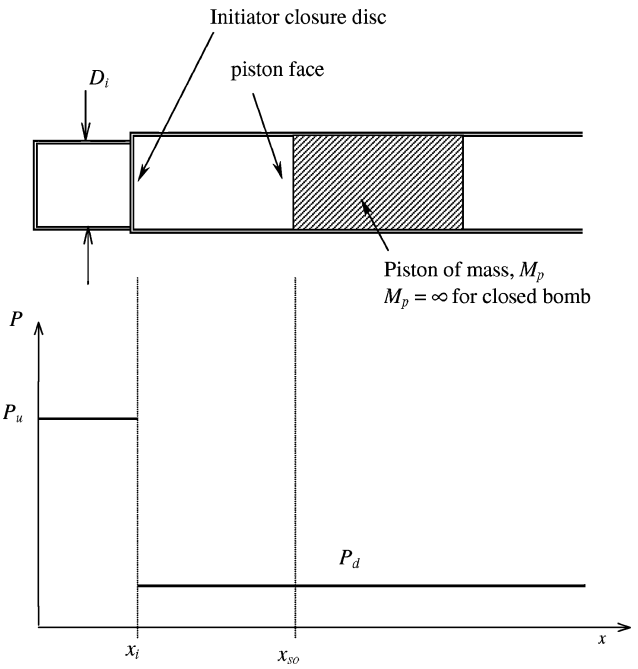

Fig. 5 Schematic diagram of a generic pyrotechnic device and initial pressure profile used in one-dimensional gasdynamics model.

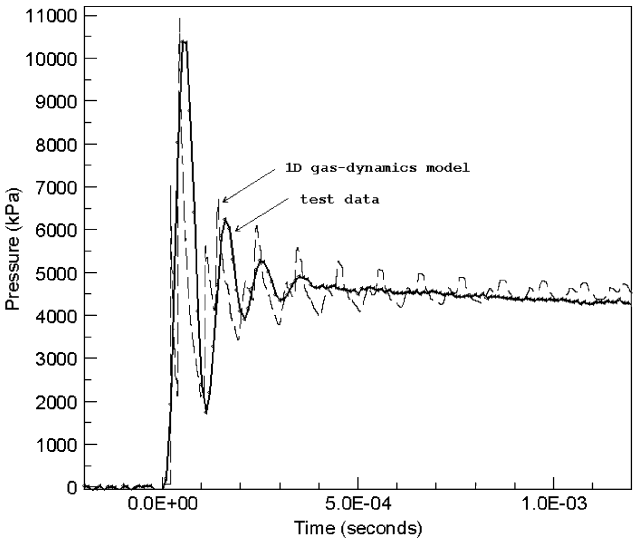

Fig. 6 Simulation of pressure vs time trace of NSI-1 initiator firing in 10-cc closed bomb using one-dimensional gasdynamics model.

The one-dimensional gasdynamics model is used to simulate the NSI-1 firing in a 10-cc closed bomb. The pressure–time result is compared to the actual test data and is shown in Fig. 6. Following are the parameters used for the simulation: $D_i = 0.74$ in. (1.88 cm), $x_i = 0.12$ in. (0.30 cm), $x_{s0} = 1.42$ in. (3.60 cm), $\mathrm{d}x = 0.01$ in. (0.025 cm), $P_u = 6730$ psi (46,400 kPa), and $T_u = 5018$ K, the adiabatic flame temperature of zirconium potassium perchlorate (ZPP), which is the main charge of the NSI-1 initiator. The values of D_i and x_{s0} are consistent with the dimensions of the actual closed bomb used for test. The value of x_i is chosen such that it represents about twice the internal volume of the actual initiator housing. This heuristically simulates a case where the disk closure ruptures before the charge completely burns out such that the effective volume in which the charge burns out is about twice the internal volume of the housing. P_u is, then, calculated:

$$P_u = (650\,\text{psi}) x_{s0}/x_i \quad (10)$$

It is seen that the one-dimensional gasdynamics model yields results that are in a fairly good agreement with the test data. The amplitude and the frequency of the fluctuating pressure are well matched in the early portion of the data. The relatively fast dissipation of fluctuations in the steady portion of the data is not well predicted by the one-dimensional model. This is a limitation inherent to one-dimensional assumption. Nevertheless, the model is in good agreement with the test data overall. Richardson's extrapolation method was applied to investigate the grid convergence of the calculations by considering three different grid sizes. For the pressure–time integral for the first 260 μs of the results, the order of convergence was 0.53; the grid-convergence indices were 6.1 and 8.9% for grid spacings 1-2 and 2-3, respectively. And the asymptotic range of convergence was 0.98.

Quasi-Equilibrium Ballistics Model

The unsteady portion of the initiator pressure output in the NSI-1 example lasts about 0.38 ms. If the unsteady portion of the initiator

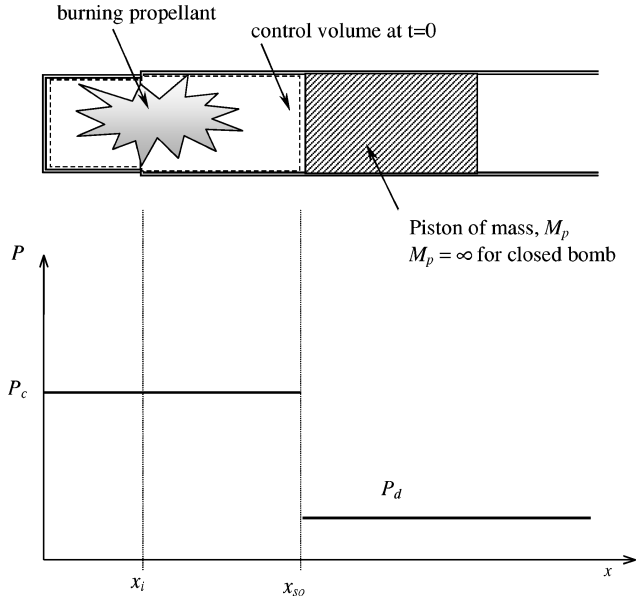

Fig. 7 Schematic diagram of a generic pyrotechnic device and pressure profile assumed in quasi-equilibrium model.

output has negligible contribution to the overall performance of a device, then a simpler quasi-equilibrium ballistic model is adequate. The main difference between the gasdynamics model and the quasi-equilibrium model is that the quasi-equilibrium model assumes zero spatial gradients of thermodynamic quantities. Whereas the gasdynamics model resolves the thermodynamic quantities at each spatial location for each time step, the quasi-equilibrium assumes that the thermodynamic quantities are spatially homogeneous for each time step. Another important difference between the two models is that the gasdynamics model neglects the finite burning process of the energetic material by assuming all energetic material is burned at time zero, whereas the quasi-equilibrium model does consider the finite burning process. The quasi-equilibrium description of the NSI-1 firing in the closed-bomb is that at time zero the closure disk ruptures and the propellant charge begins to burn in the entire 10 cc volume. At any given moment, the pressure in the closed bomb is spatially homogeneous. Figure 7 represents the quasi-equilibrium description of the NSI-1 closed-bomb firing.

In general, the quasi-equilibrium ballistics model is comprised of the following set of equations: burning-rate equation, burning-geometry equation, and the equation of state for the products of combustions, energy equation, and the rigid-body equation of motion. First, the burning rate of a solid propellant can be described empirically by Vielle's law of burning[15]:

$$\frac{\mathrm{d}\lambda}{\mathrm{d}t} = b \cdot P^n \tag{11}$$

The preceding equation relates the burning rate of a propellant to the ambient pressure in which it is burning. λ is a characteristic length that describes the geometry of the propellant charge; b and n are constants, which are inherent properties of the propellant's chemical composition. The amount of gases produced by the propellant at a given instance is related to the geometry of the propellant grain and can be expressed in a polynomial of λ:

$$m_p = m_{p_0} \sum_j k_j \lambda^j \tag{12}$$

The coefficients k_j describe the relationship between the volume of the propellant grain and λ. The combustion product gases in the chamber, where the propellants are burning, are assumed to achieve thermodynamic equilibrium at each time frame. Then, the pressure inside the chamber is described by an equation of state[15]:

$$P(V - \bar{\eta}) = m_p \bar{R} T \tag{13}$$

The equation of state takes into consideration the nonidealness of the gases by introducing a parameter η. Because the products of combustions are often mixture of gases, the thermodynamic quantities are given by the averaged mixture properties. The temperature inside the chamber is obtained from the first law of thermodynamics:

$$\frac{\mathrm{d}E}{\mathrm{d}t} = (\dot{Q} + \dot{W}) \tag{14}$$

Neglecting any potential energy contributions, E is the summation of internal and kinetic energy in the control volume. The control volume might be expanding or contracting with time as the boundaries move. The internal energy is expressed as

$$U = m_{\text{c.v.}} \cdot \int_{T_{\text{ref}}}^{T} \bar{c}_v \, \mathrm{d}T' \tag{15}$$

And the work done by or done unto the control volume is

$$W = -\int_{V0}^{V} P \, \mathrm{d}V' \tag{16}$$

If the motion of the control volume boundary is one-dimensional and the moving boundary's surface area is constant throughout its motion, then Eq. (16) can be rewritten as

$$W = -A_P \cdot \int_{x_0}^{x} P \, \mathrm{d}x' \tag{17}$$

Finally, the motion of the moving body is related to the chamber pressure by Newton's second law of motion:

$$F = M_P \cdot a = P A_P = M_P \frac{\mathrm{d}^2 x}{\mathrm{d}t^2} \tag{18}$$

Equations (11–18) can be expressed to form a system of first-order ordinary differential equations with respect to time. A conventional numerical integration technique, such as the Runge–Kutta method, can easily applied to solve the system of differential equations.[16]

The result of the quasi-equilibrium model is compared with the test data in Fig. 8. The pressure rise in the quasi-equilibrium model result reflects an estimated burning-rate of ZPP charge. The burning rate was interpolated by using an average time-to-peak pressure value made available through an existing data archive. As expected, the quasi-equilibrium model does not resolve the initial pressure fluctuations. But the model follows the overall pressure curve reasonably well in the steady region. Both the quasi-equilibrium model

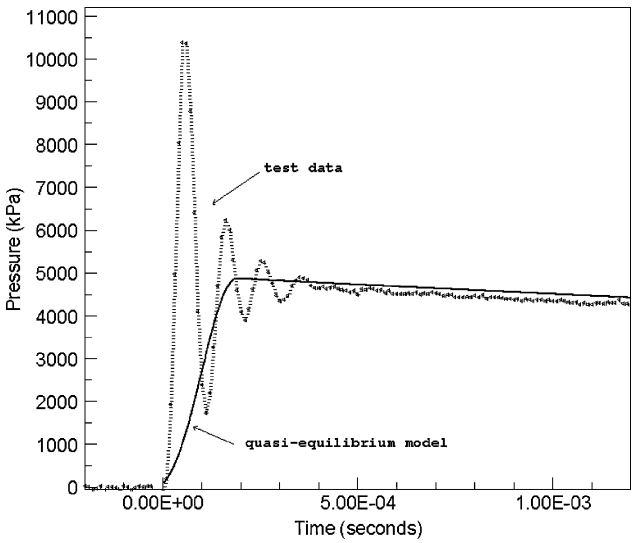

Fig. 8 Simulation of pressure vs time trace of NSI-1 initiator firing in 10-cc closed bomb using quasi-equilibrium ballistics model.

and the gasdynamics model can adequately simulate initiator performance at least in predicting the peak pressure and the time-to-peak pressure in the conventional sense. However, it is obvious from Fig. 4 that the quasi-equilibrium model will become increasingly inadequate if the unsteady phase of initiator performance plays a significant role in the overall mechanism of a device.

Normally Open Pyrotechnic Valve

Operation and Mechanics

The schematic drawing of a pyrovalve, designed to shut off a rocket engine by cutting off the fuel flow, is shown in Fig. 9. The main components that comprise the pyrovalve are 1) housing, 2) initiator, 3) piston, 4) shear-pin, and 5) end-of-stroke lock mechanism. When at normal setting, the valve is open and allows fluid to flow through a flowpath, which is located downstream of the piston. When the engine shut-off command is given, an electrical signal is sent to the initiator, which, in return, causes a rapid production of high-pressure and high-temperature gases, which, then, push on the piston. This force breaks the shear pin and sends the piston traveling to the right, which disables the fuel flow-through by sealing its passage. A piezoelectric pressure sensor is used to measure the pressure at a location upstream of the piston, at a sampling rate of 50 kHz. Also, an accelerometer is placed on the exterior surface of the valve in order to measure accelerations along the axis of piston motion. Acceleration trace is primarily used as a marker for distinct events such as the moment of bridgewire burnout, start of stroke, and end of stroke. The same data-acquisition system that was used for the NSI-1 closed-bomb test was utilized. The housing and the piston are both made of stainless steel. The piston mass M_p is 0.028 lb-mass (0.013 kg). The initial internal volume of the valve V_0 is 0.04577 in.^{3} (0.75 cm^3), and the effective internal diameter of the housing D_i is 0.172 in. (0.44 cm). The piston stroke is 0.42 in. (1.07 cm) before coming in contact with the locking mechanism. The terminal velocity with which the piston engages the locking mechanism is a crucial parameter that affects the success of the lock, as well as the structural integrity of the valve. The energetic material in the initiator is ZPP, and the initiator is designed to produce 210 ± 50 psi (1450 ± 345 kPa) in 10-cc closed-bomb, when fired in a room temperature environment.

Gasdynamics Model Simulation

The one-dimensional gasdynamics model is applied to simulate the actuation of the normally open pyrovalve. The initial pressure profile in the valve at time zero $P(x)$ is illustrated in Fig. 10a. Also the time–space diagram for the shock wave, its interactions, and the piston travel path is shown in Fig. 10b. P_u is consistent with the specific pressure specified for the initiator: $P_u = (210 \text{ psi}) \cdot (10 \text{ cc})/(\pi x_i D_i^2/4)$, where $(\pi x_i D_i^2/4)$ is the internal volume of the initiator housing. At $t = 0^+$, ZPP in the initiator burns out, and the closure disk ruptures instantaneously. This sets off a strong shock traveling to the right and rarefaction waves traveling to the left. The right traveling shock first reaches the piston face at $t = t_1$ and exerts a force at which instance the piston begins to accelerate.

The results of the gasdynamics model are shown in Figs. 11a and 11b. The following parameters reflect the initial shock profile used for the simulation: $x_i = 0.3$ in. (0.76 cm), which yields $P_u = 18{,}390$ psi (127 MPa). The value of x_i used here is greater than the actual physical dimension of the initiator housing. Again, this heuristically simulates the actual event in which the burnout of the initiator charge occurs sometime after the closure-disk ruptures. The calculations were performed with $\mathrm{d}x = 0.005$ in. (0.0127 cm) and did not include the heat-loss effect because the total heat loss during the time duration less than 60 μs will have had a negligible effect on the total mechanical output of the device. A value of $\bar{f} = 0.02$ was used in the calculations. Additional calculations with $\bar{f} = 0$ showed negligible differences. A grid-convergence investigation was carried out for the end-stroke piston velocity with three different grid sizes. The order convergence was 1.6; the grid-convergence indices were 0.05 and 0.15% for grid spacings 1-2 and 2-3, respectively. The asymptotic range of convergence was 0.999.

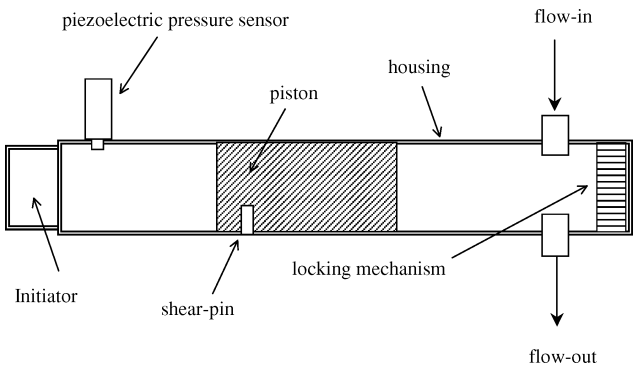

Fig. 9 Schematic drawing of normally open pyrovalve.

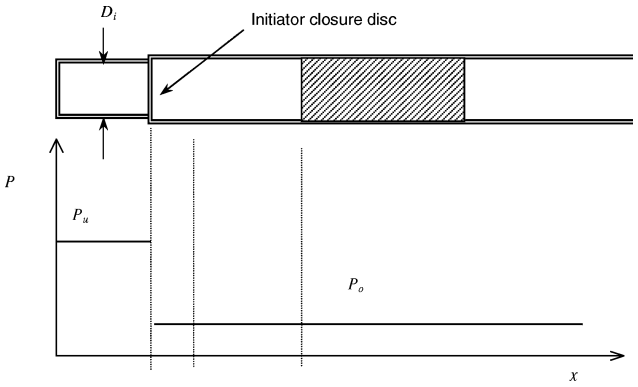

Fig. 10a Pyrovalve pressure profile at $t = 0$ used in one-dimensional gasdynamics model.

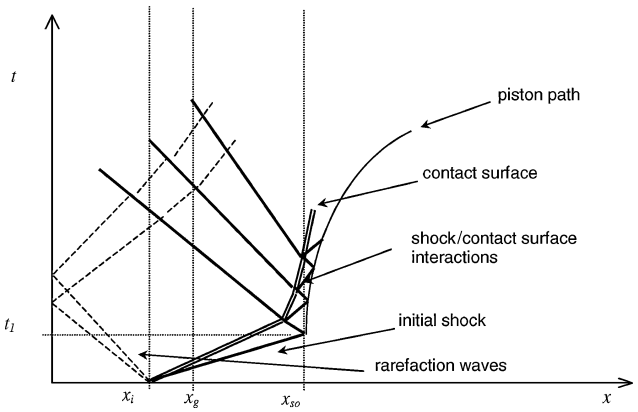

Fig. 10b Time–space diagram for ensuing shock, rarefaction waves, wave interactions, and piston travel path (not in scale).

Figure 11a shows test pressure–time data measured at $x = x_g$ with the gasdynamics model result overlaid. It is seen that the model yields a result that follows the test data relatively well. The model result exhibits a similar pressure–oscillation characteristic compared with the test data but underpredicts the stroke time: test data indicate the piston engaging the locking mechanism at about 460 μs after the first motion while the model result is at about 380 μs. Figure 11b shows the piston velocity vs piston stroke obtained by integrating the pressure–time data. The pressure–time data are easily converted to force–time data by multiplying it by the effective piston area. Integrating force–time data with respect to time and dividing by piston mass gives velocity–time information. Integrating velocity-time again with respect to time gives stroke–time information. The piston velocity at the moment of its first engagement with the locking mechanism is calculated to be 155 ft/s (47 m/s) by the gasdynamics model while the integrated value from the test data is 135 ft/s (41 m/s). This is a discrepancy of approximately 15%. The pressure–time data shown in Fig. 11a, which are used to obtain the piston velocity and stroke, are measured not at the piston face but

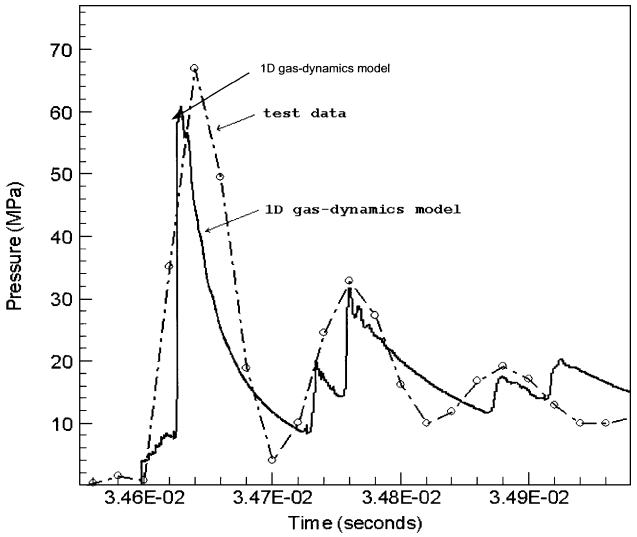

Fig. 11a Pressure vs time data of an actual firing test compared with gasdynamics model result (pressure measured at $x = x_g$).

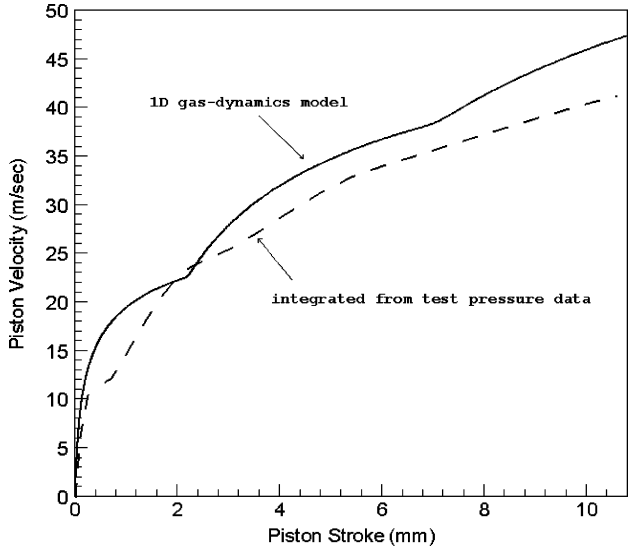

Fig. 11b Piston velocity vs piston-stroke result obtained from actual firing test compared with gasdynamics model result.

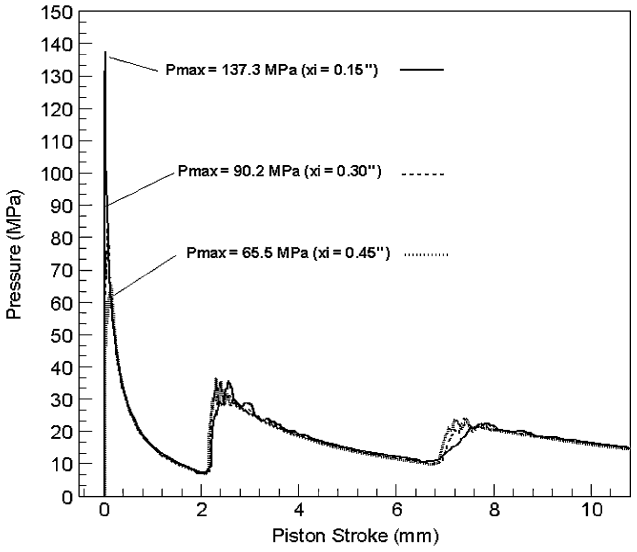

Fig. 12a Pressure at piston face vs piston stroke for $x_i = 0.15$, 0.30, and 0.45 in.

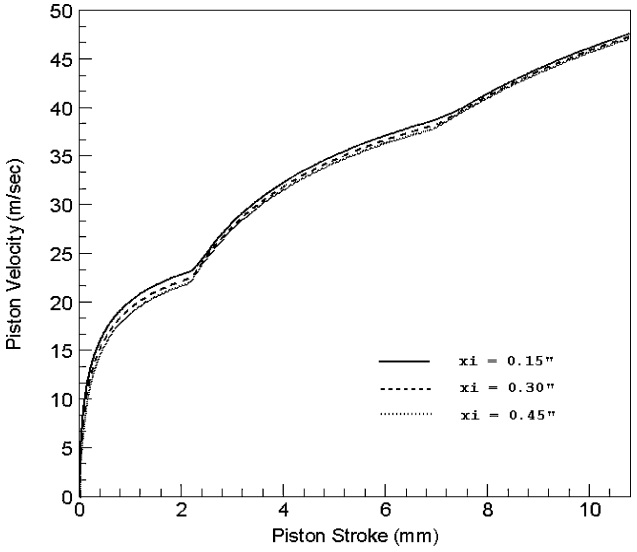

Fig. 12b Piston velocity vs piston stroke for $x_i = 0.15$, 0.30, and 0.45 in.

at x_g, some location in between the initiator and the piston face, while the numerical model calculates the piston velocity by using the pressure value at the face of the piston.

Effect of Heuristic Parameter x_i

The initial upstream pressure P_u used in the initial condition for the gasdynamics model is set by choosing the value of the heuristic parameter x_i, as shown in Eq. (9). As mentioned earlier, the gasdynamics model does not consider the finite burning process of the pyrotechnic charge in the device. In actuality, the charge might or might not complete its burning prior to the disk-closure rupture. Therefore, the initial shock strength can vary round to round depending on the timing of charge burnout vs disk-closure rupture. This variation can be simulated by decreasing or increasing the value of x_i from the known physical dimension of the initiator. The model does not have the feature to predict such variations a priori, but provides a means to estimate the effect of such variations.

To understand the effect of the heuristic parameter x_i, different values of $x_i = 0.15$ and 0.45 in. are applied and the results examined. These values yield the corresponding upstream pressure $P_u = 36{,}780$ psi (254 MPa) and 12,260 psi (85 MPa), respectively. The results are compared with the results for $x_i = 0.30$ in. Figure 12a shows the pressure at the moving piston face for all three cases plotted against the piston stroke. Figure 12b shows the piston velocity plotted against the piston stroke for all three cases. The results, as shown in the figures, indicate that the heuristic parameter x_i has a negligible effect on the final piston velocity of the normally open pyrovalve in question. A reason for the insignificant effect of x_i can be seen in Fig. 12a. The major differences in pressure for the three cases occur during the early stage of piston stroke: pressure peak = 19,950 psi; 13,190 psi; and 9510 psi for $x_i = 0.15$, 0.30, and 0.45 in., respectively. These differences quickly subside before the piston travels less than 1% of its entire stroke. Therefore, the timing effect of charge burnout vs disk rupture is deemed insignificant in the normally open pyrovalve examined here.

Quasi-Equilibrium Ballistics Model Simulation

The quasi-equilibrium model is applied to simulate the normally open pyrovalve performance. By comparing its results with those of the gasdynamics model, the unsteady effect in the pyrovalve is further illustrated. As in the closed-bomb analysis, the quasi-equilibrium model assumes that the closure disk ruptures instantaneously just prior to ignition; and therefore, the explosive charge burns, with a finite rate, in the entire available volume in the pyrovalve at all times. The model also neglects any spatial gradients of thermodynamic quantities in the valve.

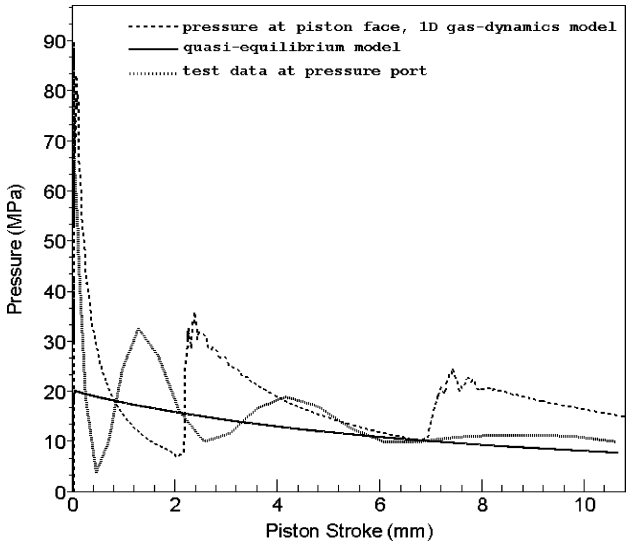

Fig. 13a Pressure vs piston stroke for quasi-equilibrium model, gas-dynamics model, and test result.

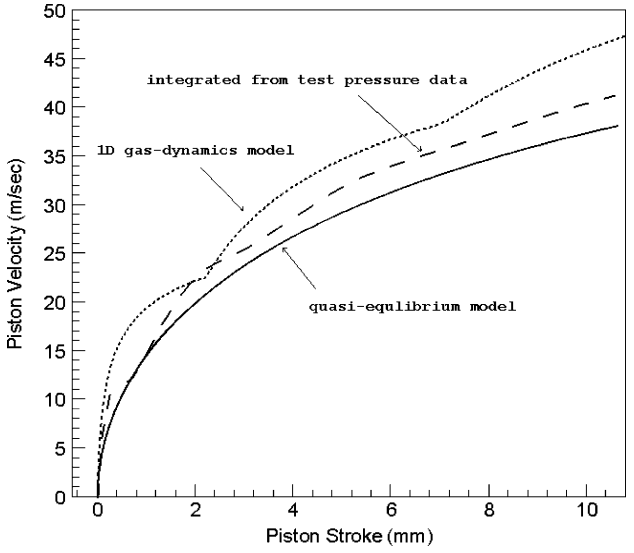

Fig. 13b Piston velocity vs piston stroke for quasi-equilibrium model, gasdynamics model, and test result.

The result of the quasi-equilibrium model is compared with the test data and the gasdynamics model results in Figs. 13a and 13b. Figure 13a shows the pressure vs piston-stroke result by the quasi-equilibrium model, and on it are the overlays of the result from the gasdynamics model (with $x_i = 0.30$ in.) and of the actual test result. Figure 13b shows the piston velocity vs piston stroke for all three cases. The results show that the quasi-equilibrium model yields results that underpredict the energy applied to the piston during actuation. The piston velocity at the moment of its engagement with the locking mechanism is 125 ft/s (38 m/s) as predicted by the quasi-equilibrium model, whereas it is 155 ft/s (47 m/s) as predicted by the gasdynamics model. This is approximately a 35% difference in kinetic energy. The result indicates that the unsteady gas dynamics plays a nonnegligible role in contributing to the performance of the normally open pyrovalve.

Critical Time Parameter

Adequacy of Quasi-Equilibrium Model

When applied to solve the dynamics of the normally open pyrovalve, the quasi-equilibrium approximation is not adequate in correctly predicting the energy output because it does not consider the large pressure fluctuation at the piston face during the unsteady phase of the actuation. However, it is not difficult to devise a scenario in which the same quasi-equilibrium model will yield acceptable results. If the actuation time of a device is much longer compared to the time it takes for the unsteady waves to reach a steady state, then the motion of the moving boundary will primarily be determined by the steady-state portion of the pressure output. Two examples are considered in order to illustrate the point. The first case, case 1, considers a pyrovalve of which the effective piston area is 20% of that of the actual pyrovalve examined in the Normally Open Pyrotechnic Valve section. The second case, case 2, considers a pyrovalve identical to that of case 1, but the internal volume is reduced to 30% of that of case 1 by decreasing the distance between the initiator closure disk and the piston face. Both cases use an initiator that is identical to the initiator used for the normally open pyrovalve. The essential parameters used for simulating cases 1 and 2 are summarized in Table 1.

Table 1 Essential parameters used for cases 1 and 2 and the normally open pyrotechnic valve

Actuator parameter	Case 1	Case 2	Normally open pyrovalve
A_p	0.023	0.023	0.109
D_i	0.172	0.172	0.172
M_p	0.028	0.028	0.028
x_{s0}	1.98	0.60	1.98
x_i	0.3	0.3	0.3
Total stroke initiator	0.42	0.42	0.42
P_{CB} in 10 cc	210	210	210
P_u	18,390	18,390	18,390

Both the gasdynamics model and the quasi-equilibrium model are applied to predict the performance of pyrovalves of cases 1 and 2. The results are shown graphically in Figs. 10a–10d. For case 1, the piston velocity at the moment of its engagement with the locking mechanism is 67.6 ft/s (20.6 m/s) as predicted by the quasi-equilibrium model, whereas it is 68.1 ft/s (20.8 m/s) as predicted by the gasdynamics model. The discrepancy in kinetic energy between the two models is less than 2%. For case 2, the velocities are 110.6 ft/s (33.7 m/s) and 110.1 ft/s (33.6 m/s), which yield a kinetic energy discrepancy of less than 1%. The reason for such agreement between the two models can easily be seen when the pressure vs stroke results are compared as shown in Figs. 14c and 14d. In both case 1 and case 2, the discrepancies in the pressure values between the quasi-equilibrium model and the gasdynamics model rapidly decrease as the stroke increases. Also, it is seen that the pressure–stroke results predicted by the quasi-equilibrium model virtually represent the averages of the results predicted by the gasdynamics model.

Dimensionless Parameter τ_c

As demonstrated by the examples, the accuracy of the quasi-equilibrium approximation increases, or the unsteady effect decreases, when the actuation time of a pyrotechnic device is long compared to a characteristic time representing the gasdynamics in the device. Therefore, a piston-dynamics time τ_D and a gasdynamics time τ_G are defined as follows:

$$\tau_D = \sqrt{S/a}, \qquad a = A_p(P_{CB}V_{CB}/V_0)/M_p \tag{19}$$

For example, $P_{CB} = 650$ psi and $V_{CB} = 10$ cc in the case of the NSI-1 initiator. Because all parameters except τ_D are known in Eq. (19), τ_D can be calculated accordingly. For the gasdynamics timescale,

$$\tau_G = 5(L_T/c_s) \tag{20}$$

where $L_T = S + x_{s0}$ and c_s is obtained from the gasdynamics relationships in Eqs. (21–23) (Ref. 17):

$$\left(\frac{c_s}{c_r}\right)^2 = 1 + \frac{2(\gamma-1)}{(\gamma+1)^2}\left[\gamma\left(\frac{W_s}{c_r}\right)^2 - \left(\frac{c_r}{W_s}\right)^2 - (\gamma-1)\right] \tag{21}$$

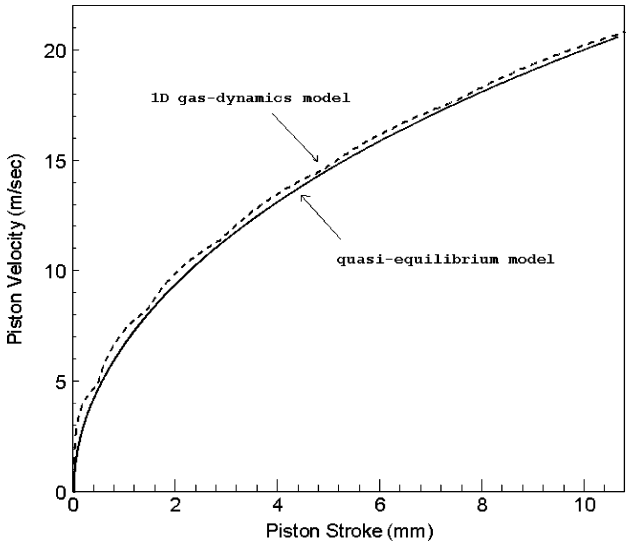

Fig. 14a Piston velocity vs piston stroke for case 1 predicted by quasi-equilibrium model and gasdynamics model.

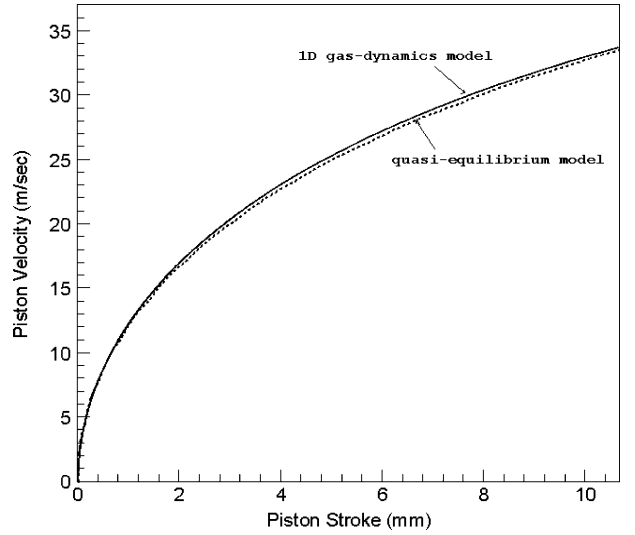

Fig. 14b Piston velocity vs piston stroke for case 2 predicted by quasi-equilibrium model and gasdynamics model.

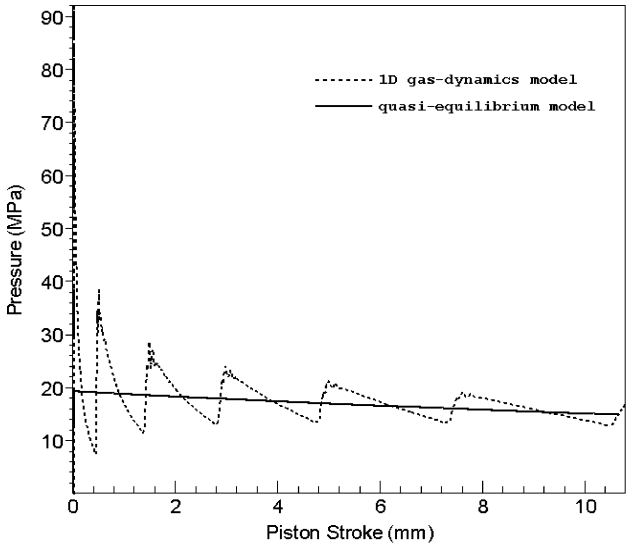

Fig. 14c Pressure at piston face vs piston stroke for case 1 predicted by quasi-equilibrium model and gasdynamics model.

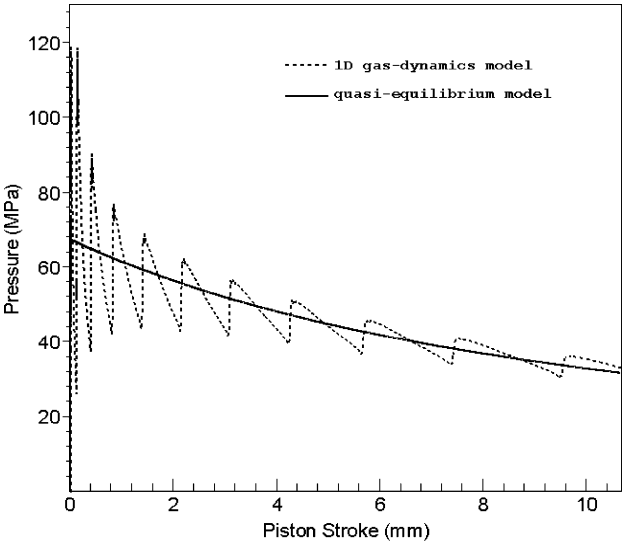

Fig. 14d Pressure at piston face vs piston stroke for case 2 predicted by quasi-equilibrium model and gasdynamics model.

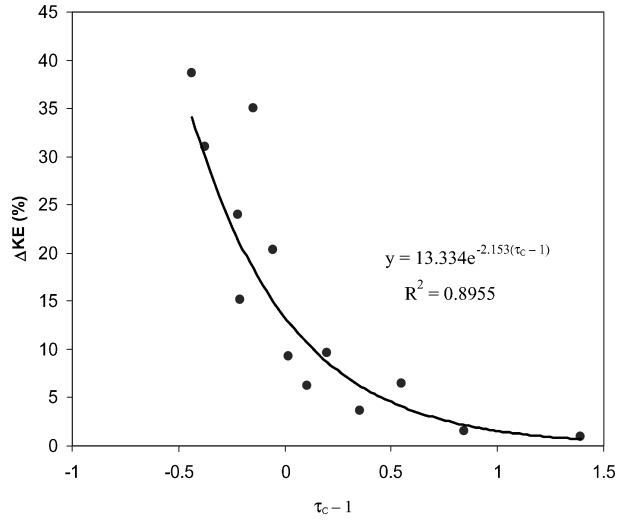

Fig. 15 Kinetic energy difference between gasdynamics model and quasi-equilibrium model plotted against the critical parameter $\tau_C - 1$.

where c_0 is the sound speed of the undisturbed fluid downstream. W_s is obtained from the following relationships:

$$\frac{p_s}{p_r} = 1 + \frac{2\gamma}{\gamma + 1}\left[\left(\frac{W_s}{c_r}\right)^2 - 1\right] \tag{22}$$

$$\frac{p_r}{p_u} = \frac{p_r}{p_s}\left(1 - \frac{\gamma - 1}{2\gamma}\frac{(p_s/p_r - 1)}{\sqrt{1 + [(\gamma + 1)/2\gamma](p_s/p_r - 1)}}\right)^{2\gamma/(\gamma - 1)} \tag{23}$$

The factor 5 in Eq. (20) is applied by considering a flow discharging through a duct from a reservoir. In such a case, a steady flow condition is approximately reached when the value ct/L is about 5 (Ref. 17). In the present case, the shock speed c_s takes the place of c, and the total stroke L_T takes the place of L. Finally, the ratio of the two characteristic times is simply defined as

$$\tau_C = \tau_D/\tau_G \tag{24}$$

The usefulness of the parameter τ_c is further investigated by considering 10 additional cases and examining the relationship between τ_c and the end-stroke kinetic energy difference between the gasdynamics and the quasi-equilibrium assumptions. The 10 additional

Table 2 Essential parameters used in cases 1–12 and the calculated values of τ_c and the kinetic energy difference between gasdynamic model and quasi-equilibrium model

Actuator parameter	Case 1	Case 2	Case 3	Case 4	Case 5	Case 6	Case 7	Case 8	Case 9	Case 10	Case 11	Case 12
A_p	0.023	0.023	0.023	0.023	0.023	0.023	0.023	0.023	0.049	0.049	0.049	0.049
D_i	0.172	0.172	0.172	0.172	0.172	0.172	0.172	0.172	0.25	0.25	0.25	0.25
M_p	0.028	0.028	0.015	0.01	0.005	0.028	0.015	0.015	0.028	0.01	0.028	0.012
x_{s0}	1.98	0.60	1.98	1.98	1.98	1.98	1.98	1.98	1.98	1.98	0.6	0.6
Total stroke initiator	0.42	0.42	0.42	0.42	0.42	0.42	0.22	0.42	0.22	0.22	0.42	0.42
P_{CB} in 10 cc	210	210	210	210	210	650	850	850	650	650	650	650
τ_C	1.85	2.39	1.35	1.10	0.78	1.20	0.62	0.79	0.95	0.56	1.55	1.01
ΔKE, %	1.5	0.9	3.7	6.3	24.0	9.6	31.0	15.1	20.3	38.7	6.5	9.3

cases were devised such that the additional values of τ_c would be derived not only by the changes in the mechanical aspects, such as the stroke distance and the internal diameter of housing, but also by the changes in the gas-dynamic aspects such as the initial upstream pressure. The parameters used for the 10 additional cases as well as cases 1 and 2 are summarized in Table 2. The results are illustrated by plotting the kinetic energy differences between the two models against the parameter τ_c as shown in Fig. 15. When the results were interpolated with an exponential fit, they yielded the following trend with a R-square value of 0.896:

$$\Delta KE = 13.3 \cdot \exp(-2.15 \cdot \tilde{\tau}_C), \qquad \tilde{\tau}_C = \tau_C - 1 \tag{25}$$

This suggests that one can expect about 13% error by the quasi-equilibrium assumption if the device in question has τ_c closed to unity and that the error will increase/decrease exponentially as τ_c decreases/increases from unity. If an "acceptable region" were to be defined as the region of τ_c under which the quasi-equilibrium assumption is expected to produce error of less than, say, 15%, then this acceptable region would be described by

$$\tau_c > 1 \tag{26}$$

Therefore, Eq. (26) suggests a limit beyond which the output energy of a pyrotechnic actuator can be approximated, with a reasonable degree of accuracy, by ignoring the unsteady gasdynamics that are present in the device.

Summary

Unsteady flow effects present in pyrotechnic actuators cannot be neglected when the device completes its stroke well before the gasdynamics in the device reaches a steady state. Therefore, a quasi-equilibrium approximation often used to predict energy output of actuators must be used with discretion, especially for actuators with relatively rapid response time. In such cases, initiator performances must be better understood and specified. The peak pressure and the time-to-peak pressure values that are usually used to specify the output energy of an initiator represent values at an equilibrium state. The unsteady pressure fluctuations which might be present in the early stage of initiator output are not usually specified even though the pressure fluctuations can have a significant effect in the mechanical energy output of an actuator, especially if the sole source of the mechanical power is the initiator.

In this paper, a simple one-dimensional gasdynamics model is developed and illustrated to be a useful tool for investigating the unsteady flow effects in pyrotechnic actuators. Even with its simplicity, the model is shown to yield good results when it is applied to simulate a firing of a NSI-1 initiator in a 10-cc closed bomb and a firing of a normally open pyrotechnic valve. The main feature of the gasdynamics model is that it assumes an instantaneous burnout of explosives in the device, which renders the problem a shock-tube problem. A model can easily be developed so that explosive burning is resolved along with the gasdynamic effects.

The gasdynamics model is, then, used to establish a nondimensional time parameter τ_c, which can be used to quickly predict whether the unsteady effect in a given pyrotechnic device can be negligible or not, where τ_c is a ratio between an estimated stroke time of the given device and the estimated time for the gasdynamics in the device to reach a steady state. It is shown that $\tau_c > 1$ represents a limit beyond which the unsteady gasdynamic effects can be neglected with a reasonable degree of accuracy.

References

[1]Hohman, C., Tipton, B., Jr., and Dutton, M., "Propellant for the NASA Standard Initiator," NASA TP-2000-210186, Oct. 2000.

[2]Bement, L. J., and Schimmel, M. L., "A Manual for Pyrotechnic Design, Development, and Qualification," NASA TM-110172, June 1995.

[3]Lee, H. S., "Modeling of High Speed Duct-flows in CAD/PAD," AIAA Paper 2000-3409, July 2000.

[4]Lee, H. S., "Modeling of Large Ballistic Retractor," AIAA Paper 2001-3770, July 2001.

[5]Vorozhtsov, A., Bondarchuk, S., Salko, A., and Kondratova, O., "Mathematical Simulation of Airbag Inflation by Low Temperature Gas Generator Products," *Propellants Explosives Pyrotechnics*, Vol. 25, No. 5, 2000, pp. 220–223.

[6]Eisenreich, N., Fischer, T. S., Langer, G., Kelzenberg, S., and Weiser, V., "Burn Rate Models for Gun Propellants," *Propellants Explosives Pyrotechnics*, Vol. 27, No. 3, 2002, pp. 142–149.

[7]Kopyoff, V., and Giedt, W. H., "Computer Design of a Pyrotechnic-Powered Self-Decelerating Actuator," American Society of Mechanical Engineers, Paper 75-DET-105, Sept. 1975.

[8]Lee, H. S., "Unsteady Dynamics of Squib-Powered Pyrotechnic Devices," *Proceedings of the Twenty-Ninth International Pyrotechnic Seminar*, edited by F. J. Schelling, IPSUSA, Denver, CO, 2002, pp. 427–434.

[9]Bement, L. J., and Multhaup, H. A., "Determining Functional Reliability of Pyrotechnic Mechanical Devices," AIAA Paper 97-2698, July 1997.

[10]"Design and Performance Specification for NSI-1 (NASA Standard Initiator-1)," SKB26100066, Rev. C, March 1990.

[11]"HT600 Operators Reference Manual," Hi-Techniques, Inc., Madison, WI, Sept. 1998.

[12]Colella, P., and Woodward, P. R., "The Piecewise Parabolic Method (PPM) for Gas-Dynamical Simulations," *Journal of Computational Physics*, Vol. 54, No. 1, 1984, pp. 115–173.

[13]White, F. M., *Fluid Mechanics*, 3rd ed., McGraw–Hill, New York, 1994, p. 318.

[14]Incopera, F. P., and DeWitt, D. P., *Introduction to Heat Transfer*, Wiley, New York, 1985, pp. 202–204.

[15]Corner, J., *Theory of the Interior Ballistics of Guns*, Wiley, New York, 1950, pp. 40, 41, 100, 101.

[16]Press, W. H., Teukolsky, S. A., Vetterling, W. T., and Flannery, B. P., *Numerical Recipes in Fortran—The Art of Scientific Computing*, 2nd ed., Cambridge Univ. Press, Cambridge, England, U.K., 1992, pp. 704–706.

[17]Shapiro, A. H., *The Dynamics and Thermodynamics of Compressible Fluid Flow*, 1st ed., Vol. 2, Ronald, New York, 1954, pp. 982–986, 1000–1002.

B. Hassan
Associate Editor